

Cooper-pair resonances and subgap Coulomb blockade in a superconducting single-electron transistor

J. J. Toppari,¹ T. Kühn,¹ A. P. Halvari,¹ J. Kinnunen,² M. Leskinen,¹ and G. S. Paraoanu¹

¹*Nanoscience Center, Department of Physics, University of Jyväskylä, P.O. Box 35 (YN), FIN-40014 University of Jyväskylä, Finland*

²*JILA and Department of Physics, University of Colorado, Boulder, Colorado 80309-00440, USA*

(Received 10 August 2007; published 21 November 2007)

We have fabricated and measured superconducting single-electron transistors with Al leads and Nb islands. At bias voltages below the gap of Nb we observe clear signatures of resonant tunneling of Cooper pairs, and of Coulomb blockade of the subgap currents due to linewidth broadening of the energy levels in the superconducting density of states of Nb. The experimental results are in good agreement with numerical simulations.

DOI: [10.1103/PhysRevB.76.172505](https://doi.org/10.1103/PhysRevB.76.172505)

PACS number(s): 74.50.+r, 73.23.Hk, 73.40.Gk

The single-electron transistor¹ (SET) and its superconducting version is one of the most versatile tools in mesoscopic physics. It has been used for extremely sensitive charge measurements,² for the construction of Cooper pair pumps and other adiabatic devices with applications in metrology,³ and more recently for building up superconducting quantum bits.⁴

The *IV* characteristics of superconducting SETs present the usual features of quasiparticle tunneling (at voltages above $2\Delta_{\text{Nb}}+2\Delta_{\text{Al}}$), Josephson-quasiparticle tunneling (at half of these values), and Josephson effect (around zero bias). These features have been thoroughly investigated by now by many groups and the physics of a charge transport at these bias voltages is well understood. However, at low bias voltages other transport processes could also become important and can alter the performance of Josephson-based devices. In this paper, we study two such processes appearing in our Nb-based SET: Resonant tunneling of Cooper pairs, and transport through states inside the gap of Nb (subgap currents).

We have fabricated Al/AIO_x/Nb/AIO_x/Al single electron transistors using a lithographic technique described elsewhere.⁵ Measurements were done using a small dilution refrigerator equipped with well-thermalized and electrically filtered measuring lines. The superconducting gaps obtained for Nb and Al ($\Delta_{\text{Nb}}=1.4$ mV, $\Delta_{\text{Al}}=0.2$ meV), and also the measured critical temperatures for Nb ($T_{C,\text{Nb}}\approx 8.0-8.5$ K), show that the films are indeed of good quality.

At voltages below the gap of Nb, a series of gate-dependent resonance peaks appears in the *IV* characteristics of the SET (Fig. 1). We interpret this as resonant tunneling of Cooper pairs, a transport phenomenon first predicted theoretically and later observed in Al symmetrically-biased superconducting SETs.⁶ Below we describe the same process for our Nb-island SETs under the asymmetric bias shown in Fig. 1. We consider a generic process in which a charge δq_1 tunnels through the left junction and a charge δq_2 tunnels through the second junction, both into the island. During the process, a charge $\delta q = \delta q_1 + \delta q_2$ is transferred into the island and a charge $\delta Q = \delta q_1 - \delta q_2$ is transferred through the external circuit in the forward direction. The change in the electrostatic free energy (including work done by the sources) associated with this process is

$$E(\delta q, \delta Q) = \frac{(\delta q)^2}{2C_\Sigma} + \frac{\delta q}{C_\Sigma}(q_0 - C_g V_g) + \frac{\delta q}{C_\Sigma} \left(C_g - \frac{C_2 - C_1}{2} \right) V - \frac{\delta Q}{2} V, \quad (1)$$

where q_0 is the initial charge of the island, C_1 and C_2 are the capacitances of the left and right junctions, C_g is the gate capacitance, and $C_\Sigma = C_1 + C_2 + C_g$. Resonant Cooper pair tunneling in superconducting SETs occurs when no energy is required for processes resulting in the transport of m Cooper pairs $\delta Q = -2me$ through the external circuit and the creation of an excess of n Cooper pairs $\delta q = -2ne$ on the island, i.e., $E(-2ne, -2me) = 0$.

The dominant processes are those involving $m = \pm 1$ and $n = \pm 1$, corresponding to a single Cooper pair tunneling through either one of the junctions.⁶ For these processes, the resonant condition describes two lattices with a cell size of $(4e/C_\Sigma) \times (2e/C_g)$ (in $V \times V_g$ plane) corresponding to odd and even values of q_0/e , and displaced with respect to each other by $2e/C_\Sigma$ along the V axis and by e/C_g along the V_g axis. During the time of an experiment, q_0 can either be fixed, in which case only one lattice pattern will appear, or it can fluctuate between odd and even values, in which case what will be measured is the overlap between the two lattices, resulting in a checkerboard lattice with half the periodicity. This last situation occurs indeed in all of our three samples. To check this, we first measured the gate modulation at voltages above the quasiparticle threshold of Nb, where the transport is of single-electron type, and determined e/C_g . This corresponds to the size of the checkerboard pattern along V_g that we see in our measurements at lower bias as well, e.g., $e/C_g = 12.3$ mV ($C_g = 12.9$ aF) for the sample of Fig. 1. (For clarity, we will concentrate our discussion on that particular sample from now on. The other two samples yielded similar results.) The observation that the checkerboard pattern is $1e$ -periodic allows us to determine $e/C_\Sigma = 68.3$ μV and thus the charging energy $E_C = e^2/2C_\Sigma = 34.1$ μeV .⁷ The SET's junction asymmetry is reflected in the different absolute values of the positive-slope lines (for which n and m have different signs) versus the negative-slope lines (m and n have the same sign), yielding $C_1 = 1.03$ fF and $C_2 = 1.29$ fF.

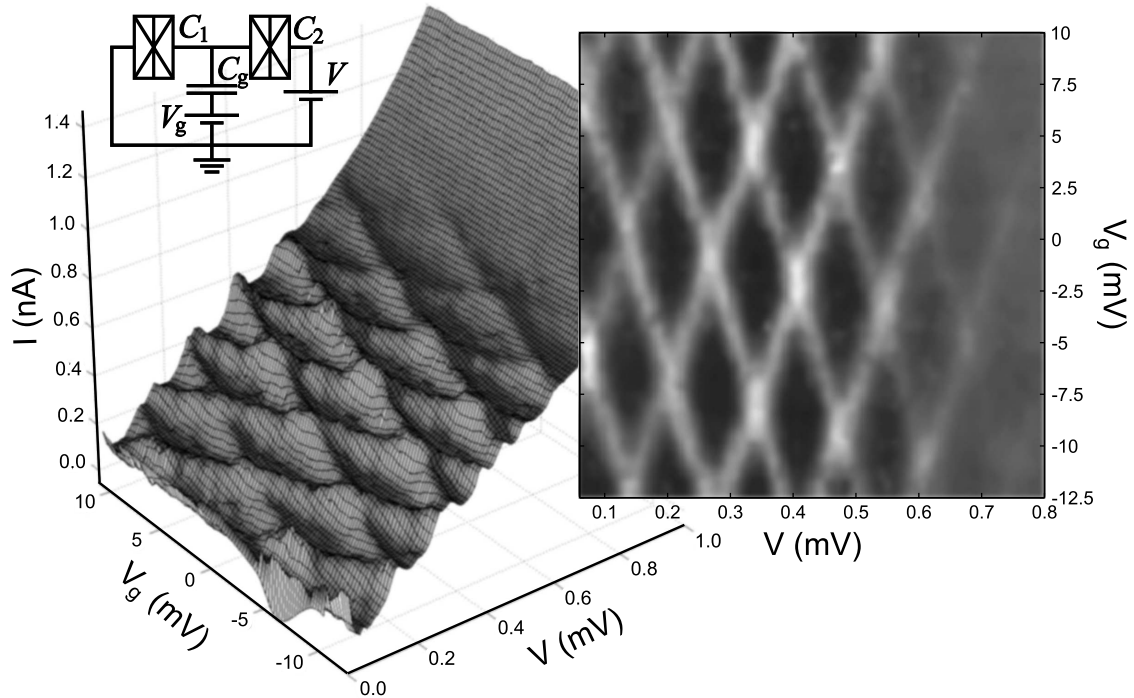


FIG. 1. Schematic of the circuit (upper left inset) and current versus bias and gate voltages (3D plot) showing the checkerboard pattern (right inset) associated with resonant tunneling of Cooper pairs. The contour plot of the right inset is obtained by subtracting the background current thus leaving only the characteristics of the resonant tunneling.

To check for consistency, we have determined E_C also by standard Coulomb-blockade thermometry⁸ with the superconductivity both in Al and Nb suppressed. We find $E_C = 36 \mu\text{eV}$, which is in very close agreement with the results above.

The second intriguing feature in the low-bias IV of our Nb-island SETs is the presence of relatively large subgap currents: From Figs. 1 and 2(a) one can see that the Cooper pair resonances appear as being built upon a current which increases with bias voltage (at voltages larger than

$2\Delta_{\text{Al}} + 2\Delta_{\text{Nb}}$, it will merge into the quasiparticle current). The origin of the subgap currents in superconductors is still a matter of intense theoretical and experimental investigations.⁹ Here, we further explore these currents by using a magnetic field to suppress the gap of Al; the transition to the normal-metal state in the leads is clearly indicated by the disappearance of the Josephson effect and of the Cooper pair resonances as seen in Fig. 2(a).

While Al is in the normal state, a very interesting feature appears at low bias voltages [Fig. 2(b)], where we observe a

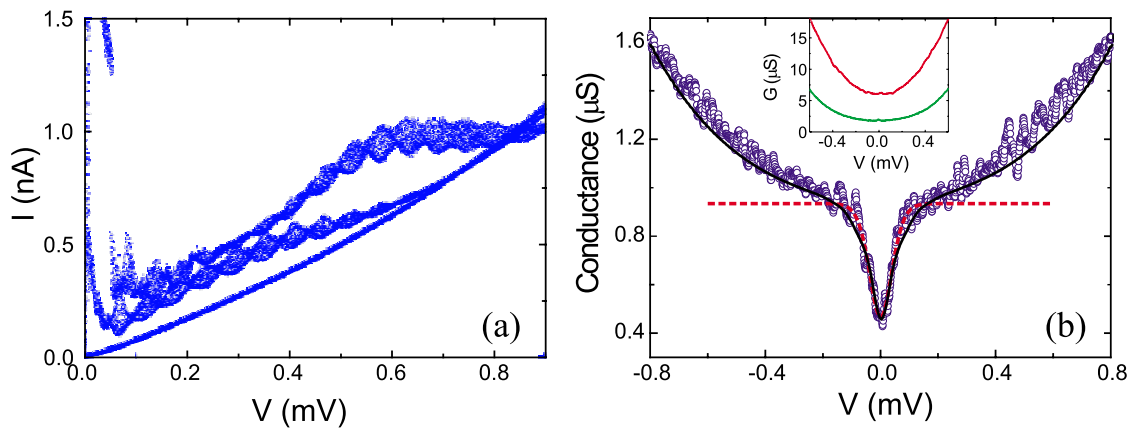


FIG. 2. (Color online) (a) Effect of a magnetic field on IV characteristics (current values at different V_g 's, showing gate modulation, are superposed): Zero, upper curve; intermediate value, middle curve; complete suppression of the gap of Al, lower curve. (b) The main graph shows the low-bias Coulomb blockade dip: Experimental values (blue), standard BCS Coulomb-blockade thermometry fit (dotted line), and the predictions of the orthodox theory with lifetime broadening and gap inhomogeneity (continuous line). The upper inset shows the conductances for two single Al-Nb junctions of normal resistances $30 \text{ k}\Omega$ (lower curve) and $11 \text{ k}\Omega$ (upper curve).

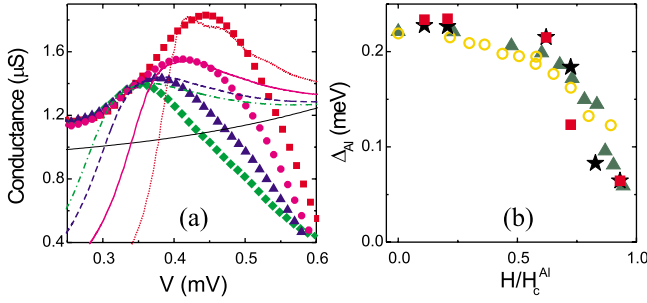


FIG. 3. (Color online) (a) Qualitative comparison between the conductances extracted from the data by averaging out the gate modulation (symbols) and those obtained by numerical simulations (lines) at different magnetic fields. (b) The gap of Al leads (open circle), measured separately, plotted together with the Al gaps determined from the conductance peaks of (a) for three SET samples (square, triangle, and star).

dip in the conductance. In measurements on single Al-Nb junctions [again with the gap of Al suppressed, Fig. 2(b) inset] this feature is not present.⁵ Instead, below 0.2 mV the IV is approximately ohmic. This shows that the dip is due to the Coulomb blockade of the subgap current, and that in the first approximation one could attempt to fit the graph with the standard analytical expressions for Coulomb-blockade thermometry⁸ (CBT) [Fig. 2(b), main graph, red dashed line]. Fitting yields $T \approx 98$ mK, which agrees well with the value measured using a calibrated resistor thermally anchored to the mixing chamber, and $E_C \approx 13 \mu\text{eV}$, which is in reasonable agreement with the value determined from Cooper pair resonances, considering that we are not in the limit $k_B T \gg E_C$ and therefore the standard approximations of Coulomb blockade thermometry are not accurate, especially for determining E_C .⁸

A better model should take into account that we are at low temperatures $k_B T < E_C$ and also describe the nonlinear increase in the subgap current at higher voltages. To develop such a model, we introduce a lifetime broadening Γ of the quasiparticle energies, resulting in a density of states¹⁰

$$\rho(E, \Delta_{\text{Nb}}) = \left| \text{Re} \left(\frac{E - i\Gamma}{\sqrt{(E - i\Gamma)^2 - \Delta_{\text{Nb}}^2}} \right) \right|. \quad (2)$$

This effect could be caused by the proximity to the metal-insulator transition, due to the granular structure of the Nb films (with our films being still on the metallic side, $\Gamma \ll \Delta_{\text{Nb}}$).¹⁰ Another possibility is the opening of conduction channels in the junctions,⁷ as suggested by the relatively large value of the room-temperature conductance [for the sample presented in Fig. 1, Fig. 2, and Fig. 3(a), this was $30 \mu\text{S}$]. Irrespective to the microscopic origin, this density of states accounts well for the existence of subgap currents seen in Fig. 2(b), inset. At low energies $E \ll \Delta_{\text{Nb}}$ the density of states can be approximated as $\rho(E, \Delta_{\text{Nb}}) \approx \Gamma / \Delta_{\text{Nb}} + (3\Gamma / 2\Delta)(E / \Delta_{\text{Nb}})^2$. In the case of a single junction of resistance R with a normal-state metal this results in a subgap conductance $R^{-1}\rho(V, \Delta_{\text{Nb}})$; therefore, ohmic for low enough voltages and increasing as V^2 for relatively larger

voltages. In addition, the granular structure of the films and, possibly, impurities resulting from outgassing of the mask polymer is also making the film inhomogeneous. As a result, the gap edge is smeared due to local fluctuations in the effective electron-electron interaction. Other fabrication techniques [e.g., the use of stronger polymers such as PES (Ref. 11)] could improve the quality of the Nb films. For our samples, since the superconducting coherence length in bulk Nb is only $\xi_{\text{Nb}} = 38$ nm, we expect to be in the limit in which the size of the inhomogeneities is much larger than ξ_{Nb} . In this case, it has been shown¹² that the effective (average) density of states takes the form

$$\bar{\rho}(E) = \int_0^\infty d\Delta_{\text{Nb}} \mathcal{P}(\Delta_{\text{Nb}}) \rho(E, \Delta_{\text{Nb}}), \quad (3)$$

where \mathcal{P} is the probability density associated with a certain value of the gap. For small levels of inhomogeneity, the function \mathcal{P} is a Gaussian of standard distribution σ centered around an average gap value (slightly smaller than the bulk value).

Finally, to complete our model, we calculate numerically the currents and conductances for the superconducting SET in the framework of the orthodox theory of sequential tunneling, by computing the tunneling probabilities into and out of the island (with the density of states above for Nb) and by solving the master equation for the charge on the island. In the case of suppressed Al gap, a very good fit is obtained for $\sigma = 0.38$ meV, $\Gamma = 37.5 \mu\text{eV}$, $T = 95.7$ mK, and charging energy, $E_C = 34.1 \mu\text{eV}$, as determined before [Fig. 2(b), main graph, continuous line]. The temperature also agrees well with the value obtained by simple CBT fitting above and the value of the thermometer.

In the case when the leads are superconducting the comparison with the experimental data can be done only qualitatively: the main reason is the existence of Cooper pair resonances, yielding an extra contribution to the current which cannot be eliminated in a straightforward way. However, a number of qualitative features can still be observed by averaging the resonance peaks over gate voltages. The conductances obtained by this procedure should reflect the voltage dependence of the subgap current in the region where the height of the resonance peaks is approximately constant. A reasonably fair qualitative agreement with the model presented above is obtained [Fig. 3(a)]. The main feature that we see both in the calculated conductivities and in the conductivities obtained from our data through the above procedure is the appearance of a peak at the onset of the Al quasiparticle threshold ($2\Delta_{\text{Al}}$). By using a magnetic field to partially suppress the gap of Al, we see that the peak moves to the left [see Fig. 2(a) and Fig. 3(a)]. To verify that this is indeed the case, we have measured single Al-Al junctions with the same fabrication parameters as the leads of the Nb-island SET, and determined the gap of Al at various magnetic fields [Fig. 3(b), circles]. The agreement with the gaps determined from the low-voltage features [Fig. 3(a)] of three Nb-island SET samples (square, triangle, star) is good.

In conclusion, we have fabricated and measured superconducting single-electron transistors and we have presented

evidence for a number of transport processes occurring at bias voltages below the gap of the island: resonant tunneling of Cooper pairs, Coulomb blockade of the subgap current for normal leads, and the appearance of a step in the subgap current at $2\Delta_{AI}$ for the case of superconducting leads.

This work was supported by the Academy of Finland (Acad. Res. Grant No. 00857 and Projects No. 7111994,

7118122, 7205476), EU (IST-1999-10673, HPMF-CT-2002-01893), and the Finnish National Graduate School in Materials Physics. J.K. acknowledges the support of the Department of Energy, Office of Basic Energy Sciences via the Chemical Sciences, Geosciences, and Biosciences Division. G.S.P. would like to thank D. V. Averin, Yu. V. Nazarov, and I. S. Beloborodov for useful discussions.

-
- ¹*Single Charge Tunneling*, edited by H. Grabert and M. H. Devoret (Plenum, New York, 1992).
- ²R. J. Schoelkopf, P. Wahlgren, A. A. Kozhevnikov, P. Delsing, and D. E. Prober, *Science* **280**, 1238 (1998); M. H. Devoret and R. J. Schoelkopf, *Nature (London)* **406**, 1039 (2000).
- ³J. P. Pekola, J. J. Toppari, M. Aunola, M. T. Savolainen, and D. V. Averin, *Phys. Rev. B* **60**, R9931 (1999); M. Keller, A. L. Eichenberger, J. M. Martinis, and N. M. Zimmerman, *Science* **285**, 1706 (1999); A. O. Niskanen, J. P. Pekola, and H. Seppä, *Phys. Rev. Lett.* **91**, 177003 (2003).
- ⁴Y. Nakamura, Y. A. Pashkin, and J. S. Tsai, *Nature (London)* **398**, 786 (1999); D. Vion, A. Aassime, A. Cottet, P. Joyez, H. Pothier, C. Urbina, D. Esteve, and M. H. Devoret, *Science* **296**, 886 (2002); Yu. A. Pashkin, T. Yamamoto, O. Astafiev, Y. Nakamura, D. V. Averin, and J. S. Tsai, *Nature (London)* **421**, 823 (2003); T. Yamamoto, Yu. A. Pashkin, O. Astafiev, Y. Nakamura, and J. S. Tsai, *ibid.* **425**, 941 (2003); T. Duty, D. Gunnarsson, K. Bladh, and P. Delsing, *Phys. Rev. B* **69**, 140503(R) (2004); H. Zangerle, J. Könmann, B. Mackrodt, R. Dolata, S. V. Lotkhov, S. A. Bogoslovsky, M. Götz, and A. B. Zorin, *ibid.* **73**, 224527 (2006).
- ⁵N. Kim, K. Hansen, S. Paraoanu, and J. P. Pekola, *Physica B* **329-333**, 1519 (2003); G. S. Paraoanu and A. Halvari, *Rev. Adv. Mater. Sci.* **5**, 292 (2003).
- ⁶A. M. v. d. Brink *et al.*, *Z. Phys. B: Condens. Matter* **85**, 459 (1991); D. B. Haviland, Y. Harada, P. Delsing, C. D. Chen, and T. Claeson, *Phys. Rev. Lett.* **73**, 1541 (1994).
- ⁷P. Joyez, V. Bouchiat, D. Esteve, C. Urbina, and H. H. Devoret, *Phys. Rev. Lett.* **79**, 1349 (1997).
- ⁸J. P. Pekola, K. P. Hirvi, J. P. Kauppinen, and M. A. Paalanen, *Phys. Rev. Lett.* **73**, 2903 (1994).
- ⁹A. V. Balatsky, I. Vekhter, and J.-X. Zhu, *Rev. Mod. Phys.* **78**, 373 (2006).
- ¹⁰R. C. Dynes, J. P. Garno, G. B. Hertel, and T. P. Orlando, *Phys. Rev. Lett.* **53**, 2437 (1984); M. Kunchur, Y. Z. Zhang, P. Lindenfeld, W. L. McLean, and J. S. Brooks, *Phys. Rev. B* **36**, 4062 (1987); J. P. Pekola, T. T. Heikkilä, A. M. Savin, J. T. Flyktman, F. Giazotto, and F. W. J. Hekking, *Phys. Rev. Lett.* **92**, 056804 (2004).
- ¹¹P. Dubos, P. Charlat, Th. Crozes, P. Paniez, and B. Pannetier, *J. Vac. Sci. Technol. B* **18**, 122 (2000); R. Dolata, H. Scherer, A. B. Zorin, and J. Niemeyer, *Appl. Phys. Lett.* **80**, 2776 (2002); R. Dolata, H. Scherer, A. B. Zorin, and J. Niemeyer, *J. Appl. Phys.* **97**, 054501 (2005).
- ¹²A. I. Larkin and Y. N. Ovchinnikov, *Sov. Phys. JETP* **34**, 1144 (1972); A. Ghosal, M. Randeria, and N. Trivedi, *Phys. Rev. B* **65**, 014501 (2001); A. V. Balatsky, I. Vekhter, and Jian-Xin Zhu, *Rev. Mod. Phys.* **78**, 373 (2006).